Acta Astronautica 206 (2023) 72–88

Contents lists available at ScienceDirect

Acta Astronautica

journal homepage: www.elsevier.com/locate/actaastro

Research paper

An assessment of different relay network topologies to improve Earth–Mars communications

Paula Betriu [a,*], Manel Soria [a], Jordi L. Gutiérrez [a], Marcel Llopis [b], Antoni Barlabé [c]

[a] Department of Physics, Universitat Politècnica de Catalunya, 08222 Terrassa, Spain
[b] Jet Propulsion Laboratory, 91109 Pasadena, USA
[c] Signal Theory and Communications Department, Universitat Politècnica de Catalunya, 08034 Barcelona, Spain

ARTICLE INFO

Keywords:
Earth–Mars communications
Solar conjunctions
Lagrange relays
Pearl constellation
Deep Space Network

ABSTRACT

The future of deep space communications encompasses a challenging situation where the current facilities used to communicate with different spacecraft may become saturated as a result of an increasing number of missions and their complexity. From this forecast, the present study intends to provide a solution to saturation problems through strategically-located upgradable relays for Earth–Mars communications. The foremost goal of this paper is to quantitatively uncover the potential enhancements coming from relay placement in strategic orbits between Earth and Mars. Herein, two relay configurations – a.k.a. network topologies – are analyzed: the Lagrange-relays network topology and a circular, homogeneously-distributed satellite constellation, acknowledged here as *pearl constellation*. The first uses the Earth–Sun system Lagrange points L_3, L_4 and L_5 as potential locations for the relays, whilst the second defines an optimized orbit between Earth and Mars with 3 or 4 relay satellites.

To aid in the analysis, the authors developed an open-sourced piece of software that obtains the link availability as well as the data rate at which two nodes may communicate, taking as a reference the Deep Space Network (DSN) for Earth, and the Mars Reconnaissance Orbiter for Mars. For complex topologies with more than two communicating nodes, the software outputs the end-to-end bit rate and optimal communication route at each time step. Moreover, this product is extensible to analyze and optimize any network topology and could be adapted to be used for contact management and mission planning in the future.

The results show that the network-topology proposals are an advantageous option to significantly increase the link availability of Earth–Mars communications. Nevertheless, the Direct-To-Earth (DTE) link always outperforms the multi-hop path due to the limited telecommunication system's capabilities of both the spacecraft and the relays. As a result of this, the study includes an analysis on the requirements of the relay's design in order to make the constellation a beneficial and comparable alternative to the DTE link. This way, the proposed network topologies become a suitable option whom to share with the DSN communications workload, providing enhanced bit rates and data volumes as well as higher availability of the communication.

1. Introduction

Long-range space communications – also known as deep space communications when at least one of the links is beyond the cislunar space – are key to determine the success of a deep space mission.

Prospective endeavors in the space exploration arena reveal a challenging scenario for future deep space communications [1,2]. Namely, at the dawn of an epoch where more deep space missions will be launched and crewed missions are being revisited, we can expect a significant increase on the communication network's requirements. Furthermore, it is known that greater scientific knowledge redounds in more specific and complex queries, requiring more demanding technologies and data to obtain answers for those. As per the stated, this envisioned future shall address an increase on the communication network's demand. Subsequently, there shall be a consideration for improved capacity that includes: higher (1) data rate, (2) data volume, (3) number of link supports and (4) spacecraft-ground station communication availability.

More specifically, this paper focuses on the oncoming Mars exploration –both robotic and human– and its implications for future

* Corresponding author.
E-mail addresses: paula.betriu@upc.edu (P. Betriu), manel.soria@upc.edu (M. Soria), jordi.gutierrez@upc.edu (J.L. Gutiérrez), marcel.llopis@jpl.nasa.gov (M. Llopis), antoni.barlabe@upc.edu (A. Barlabé).

https://doi.org/10.1016/j.actaastro.2023.01.040
Received 14 September 2022; Received in revised form 26 January 2023; Accepted 30 January 2023
Available online 1 February 2023
0094-5765/© 2023 The Author(s). Published by Elsevier Ltd on behalf of IAA. This is an open access article under the CC BY-NC-ND license (http://creativecommons.org/licenses/by-nc-nd/4.0/).

telecommunications in radio-frequency (from now on, RF) bands. First of all, the prospects of future human exploration on Mars include higher forwarding rates in an effort to accommodate voice and video coming from or going to Earth. External communications in crewed missions are essential not only in terms of mission support but also as an emotional and social backup, as relationships and interactions in isolated, confined and extreme environments may lead to different type of conflicts within a team [3]. Second, the high ratio between the maximum and minimum distances between Earth and Mars (≈7.3) causes communication to bear significant and inconvenient differences of the data rate – in its sequential adjustment over a changing distance –, along the synodic period of Mars. Finally, communication in the framework of human exploration must be ensured 24/7 in order to reduce the mission risk, meaning that uptime is of the utmost importance. This has a direct impact on superior solar conjunctions: a period where the relative positions of the transmitter and receiver cause the Sun to interfere the normal communication –either by physical occultation or Radio Frequency Interference (RFI).

Despite the extensive analysis of solar interference [4,5], there is no established protocol to determine the proper bit rate at which communication can be held during a solar conjunction. Rather, information is transmitted at an adequate bit rate –determined through previous experience.[1] The range of positions where solar conjunctions occur is determined by the angle between the direction vectors of the observing node to the Sun and the observing node to the target, acknowledged as Sun-Target-Probe angle (hereafter referred to as STP angle, and, for communications with Earth, as Sun-Earth-Probe, SEP). According to [6], the minimum SEP angle below which a solar conjunction is considered to start with Mars is 5°. Sometimes, the SEP angle can reach values so low that the interference is unbearable, which leads to the disruption of the communication. Therefore, over the time period where SEP < 5°, which can take up to about a month, communication with Mars can be either conducted at a lower bit rate or even interrupted. This is especially critical for the Martian landers, as their sequences are planned with a shorter-term horizon when compared to orbiters, whose activities may be determined well in advance, and their science activities are heavily restricted in order to protect their assets from damage, e.g. temporally shutting down some instruments. Therefore, this time period needs to be accurately planned and agreed with the respective mission communication teams, which also takes up a considerable amount of time – up to several months – in order to draw a suitable communication schedule, given the command moratorium [7].

Last but not least, still within the Martian human exploration framework, an additional consideration would be made for the fact that one or more ground stations could become unexpectedly unavailable, disrupting communication with the crew for several hours a day. This would imply a significant risk for the mission, as the crew would be left with no mission support, and could jeopardize the schedule of activities or result in loss of data. Likewise, this is also a very undesirable situation for unmanned missions, as it has been seen with the solar conjunction event.

In order to address this challenging scenario, some researchers have proposed resorting to deep space relays, building a new network topology that could enhance at first instance the availability of the communication despite solar conjunctions or possible disruptions in the network, as well as increasing data rate and volume.

As a matter of fact, the idea of deploying relays for improved communications with deep space missions dates back to the Apollo missions, where a relay satellite was proposed at the Earth–Moon L_2 libration point in order to ensure the continuity of the communication when either the command module or the lunar excursion module were on the far-side of the Moon [8]. Still, the location of relays at the Lagrange points – a.k.a. Lagrange relays – remains a matter of today's discussions in the face of this oncoming stage of space exploration [9].

Acknowledging future needs and requirements in the long-range communications framework, some authors have included the libration points of different systems – e.g., the Earth–Sun system – on the roadmap; either to cope with solar conjunctions, space attenuation (distance) or both [10,11]. Others have gone one step further and studied the effects of such a network topology from the availability and link performance points of view. This is the case with Breidenthal, Jesick et al.[12]. From the first point of view, the authors conclude in their study that the Sun–Mars system L_4 and L_5 points are the optimal solution to provide with enhanced and continuous Earth–Mars communication. From the second point of view, however, the designed deep space relay to be located at the aforementioned Lagrange points is heavily constrained by its premise to keep it small (75-cm dish antenna) in order to reduce volume and costs. As a result, and even though the multi-hop network also involves an enhanced Martian communications relay, the RF link may not provide any more than 185 kbps, and the authors do not consider either the analysis of improved relay capacities in the RF links. On the other side, Modenini et al. [13] reveal promising results when analyzing the link capacity of a network topology that locates relays in the Earth–Sun system L_4 and L_5 points as well as an additional relay in geostationary orbit. The authors focus on the improvements obtained by increasing the frequency of the communication link to Ka-band and optical, while this study intends to stay in state-of-the-art usages of X-frequency bands and accurate models of downlink rates gathered by means of the DSN.

Aside from the telecommunications aspect of the problem, some authors have focused on the astrodynamics approach of such a network topology. This is the case with Strizzi et al. [14], who discussed the orbit design, feasibility and stationkeeping costs of an Earth–Mars communication network based on the Sun–Mars system L_1 and L_2 points; or Jesick [15], who demonstrated that a single relay spacecraft located at an Earth–Sun or Mars–Sun libration points is enough to guarantee continuous Earth–Mars communications, building an effective solution to avoid solar conjunctions. In a different scenario, Rahman et al. [16] discoursed upon the possibility of creating a new network topology based on the L-points of different systems (Earth–Moon, Earth–Sun, Mars–Sun, etc.), which eventually may lead to the significant shrinkage of the spacecraft relays and, ideally, the improved operation of *CubeSats* throughout the Solar System. Their analysis is also focused on orbit design, architecture and concept of operation.

Interestingly enough, Lagrange points may have other purposes besides deep space communications. For instance, in the network architecture domain, Wan et al. [17] and also Jiang et al. [18] have considered the benefits of using Lagrange relays as backbone nodes between subnetworks (clusters of satellites according to their link features), whilst elaborating a complex large-scale Solar System interplanetary communication network. Also, Limaye et al. [19] have analyzed the suitability of these strategic locations for a cost-effective mission that could perform science experiments or provide with advantageous fields of view for observation purposes (in the case of L_1 and L_2). On the whole, it is safe to say that Lagrange points have been widely framed in the future of deep space communications, and the motivations and uses are not exclusive.

Besides Lagrange points, another option that has received attention involves the location of a deep space relays constellation in one or more heliocentric orbits. This implementation, acknowledged in this study as pearl constellation, could also meet the improved capabilities – even outperform those – and versatility of the aforementioned Lagrange-relays network topology; with an increase in redundancy at the expense of higher costs.

To build such network topology, the number of orbits, their size and the number of satellites per orbit must be defined. One of the most-used strategies consists of placing the relays on an orbit coincident with Earth's. Howard [20] proposed placing up to three relay satellites,

[1] Personal communication with Jim Taylor.

which, along with Earth's DSN ground stations, would provide the pearl constellation with four communicating nodes in a 90° phase shift. The author analyzes the optimal design and relay cost in order to make the network topology link performance match that of the Direct-To-Earth (hereinafter referred to as DTE) link, in such a way that the DSN is able to support other deep space exploration missions rather than the ones that will most likely take over the DSN's load in the future –i.e. Moon and Mars. To do so, the relay shall be equipped with a 31 m antenna with an equivalent isotropic radiated power (EIRP) of 120 dBW, an option that, according to the author, could be practicable in the short-term future. This paper, however, does not consider the optimization of the orbit to maximize the total bit rate nor the actual availability of the communication, even though the location of the relays is assumed to minimize the effect of occultations. A different strategy consists of using orbits with different size and number of satellites. Haque [21] analyzes the performance of a very large constellation of 375 satellites in different heliocentric orbits, each of which carrying a 20 m antenna communicating via the Ka-band. This could allow for a data rate of 1 Gbps between Earth and Mars, a value that is 3 orders of magnitude above the current downlink rates and thus might be more suitable for the long-term future needs of deep space communications. Moreover, such a remarkable bit rate demands an equally ambitious relay system deployment: the total number of satellites – arbitrarily chosen – is quite significant; this would imply a considerable allocation of resources, in addition to the cascading complexity of such an orbit topology. Finally, Wan et al. [22] develop an accurate design regarding orbit size and number of satellites per orbit, setting a maximum hop distance of 0.7 AU and different optimization criteria: shortest path, minimum hops and minimum nodes. The link performance is based on additive white Gaussian noise (AWGN) channels.

Finally, some researchers have merged both strategies and built a hybrid network topology, involving both Lagrange relays and the pearl constellation. This is the case of Bhasin et al. [23], whose design involves the Earth–Sun, Mars–Sun and Jupiter–Sun libration points plus 2 augmentation relays located in a heliocentric orbit coincident with Earth's. By means of large antennas and upgraded microwave technologies that could improve gains and transmitter powers in the future, a bottleneck of at least 10 Mbps could be guaranteed in both the Martian and Jovian communication networks. Nevertheless, the authors do not indicate the underlying communication models that justify their link analysis nor delve into the potential availability improvements of the communication.

Altogether, the underlying assumption of both the Lagrange relay network and the pearl constellation is that the overall communication link between Earth and Mars can be enhanced by means of placing relays between these bodies and the consequent reduction of space losses. Moreover, the location of the relays may satisfy the off-solar constraints during conjunctions, enabling the adequate communication in those periods. Fig. 1 shows a depiction of the different network-topology configurations assessed in the present study.

In a different line of research, other approaches to improve communications in space include the implementation of an interplanetary space network – a.k.a the Future Internet –, in which a new architecture – the Delay- and Disruption Tolerant Network (DTN) – could enable the temporary storage of messages between hops; unlike the kind of end-to-end connectivity where communication is consecutive and almost immediate in time [24]. This new protocol could help cope with the existing space communication handicaps such as high latency or limited bandwidth [24]. Routing – i.e., choosing the best path according to some parameter – is an important issue in DTN design and there are different – multiple – methods to approach it. It is expected that the synergy between the construction of a new network topology and the implementation of a Space Internet could lead to meaningful improvements in the future –even better than the two methods set aside. This paper focuses on the first approach, leaving the door open for future implementations of DTN routing algorithms.

To summarize, all of the above shows that both the Lagrange-relays and the pearl constellation topologies present great potential to lead future deep space communications towards upgraded capacity levels. Nevertheless, the current picture of these network topologies, using state-of-the-art technologies, and how this relates to future relay capability upgrade needs remains unclear. Accepting the latter, one of the objectives of this study is to provide an accurate description of both the present and the future of interplanetary-relayed communications in terms of:

- Communication availability
- Bit rate and data volume

In order to achieve these goals, the authors developed an open-sourced Object-Oriented Java software tool,[2] which underwent testing with data mined from the Deep Space Network (DSN). This software, named *SolarCom* enables an assessment of potential enhancements – in terms of data rate, data volume and the avoidance of solar conjunctions – for different network topologies that may involve ground stations, spacecraft and relay satellites. This is accomplished by computing the accurate evolution of attainable bit rates and link availability over time. The relay satellites may be designable and equipped with one or two antennas, which, in turn, determine the communication strategy. Furthermore, *SolarCom* obtains, through a routing algorithm, the best end-to-end communication route at each time iteration considering link availability and bit rate.

As a matter of fact, this tool has been developed to analyze the Lagrange-relays and pearl constellation topologies, but may be extensible to any other topology design, given the satellites ephemerides over time. Additionally, it can also be used to optimize relay orbit design in terms of availability or bit rate, as it has been applied in this study for the pearl constellation orbit size determination.

Hence, this paper focuses on analyzing the capacity, when compared to the DTE link, of the proposed network topologies, assuming state-of-the-art technologies for the built-in relays. As a follow-up, this present scenario serves as a baseline to analyze what improved capacities should the relay possess in order to meet the current maximum capacity of deep space communications. The link transfer model that enables computing availability, bit rate and optimal route for the communication between two nodes is described in Section 2. Both proposed network topologies are presented and explained in Section 3 and their results are going to be discussed and compared later in Section 4. Finally, a summary of the conclusions that resulted from the outcome of this study is made in Section 5.

2. The link transfer model

This study intends to analyze the communication within the framework of a multi-hop network, i.e., with multiple contacts between different communicating nodes. At the two-node level, the link transfer model returns the bit rate at which two nodes can communicate during a certain time period. To do so, the model checks communication availability during such time interval and computes the subsequent bit rate $R(t)$. At the end-to-end path level, the model evaluates the map of available communicating nodes at each time step and finds the optimal path that provides the best overall bit rate. Therefore, in that order, the link transfer model performs three main operations:

(1) Builds the contact plan,
(2) Assesses link performance,
(3) Optimizes route.

[2] https://github.com/alcjor/solarcom.git

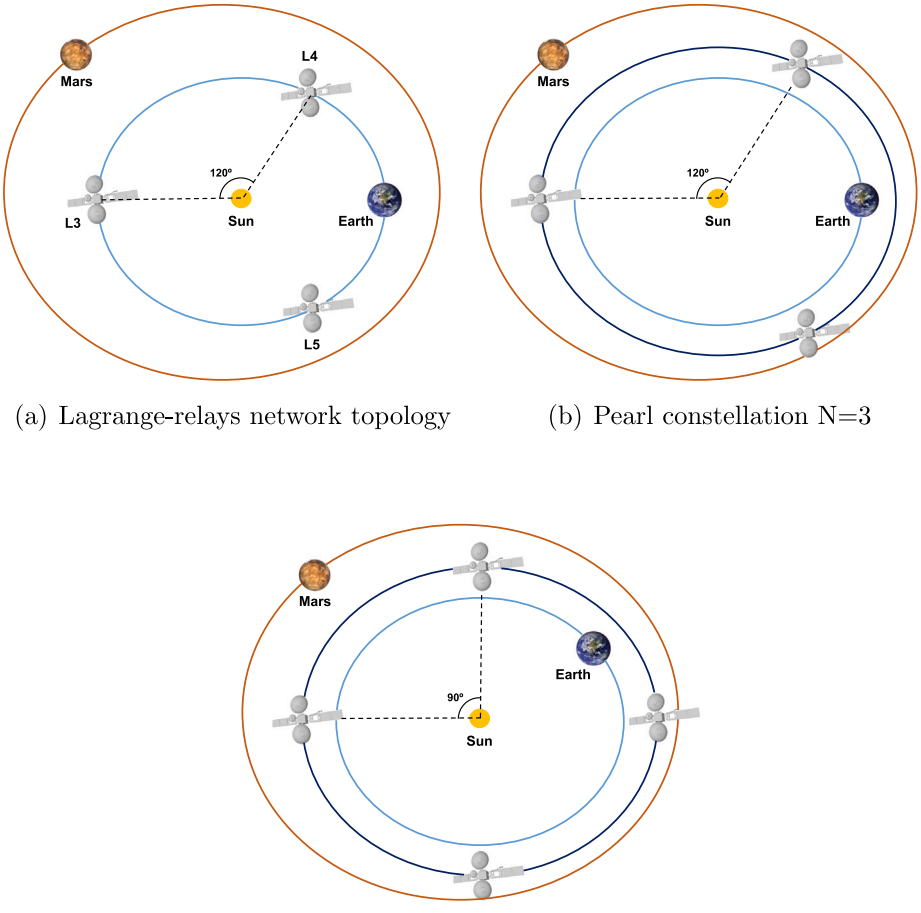

(a) Lagrange-relays network topology (b) Pearl constellation N=3

(c) Pearl constellation N=4

Fig. 1. Diagram of the different network-topology configurations analyzed in this study.

Table 1
Summary of DSN antennas included in the software.

Facility	34 m	70 m
Goldstone, USA	DSS-15	DSS-14
Canberra, AU	DSS-45	DSS-43
Madrid, ES	DSS-65	DSS-63

To compute these, information about the spacecraft, planetary bodies and ground stations is retrieved via SPICE,[3] [25] an observation geometry system – owned by NASA and managed by its Navigation Ancillary Information Facility (NAIF) – with which one can access relevant ancillary information to compute specific geometric events and its parameters at selected times.

Using SPICE kernels and modules, the authors have developed an open-source Object-Oriented Java program that addresses the above-mentioned three main problems in order to ultimately obtain the total bit rate of communication between a source – e.g., a spacecraft – and a destination –e.g., a ground station. In the following sections, the underlying physical models and the insights of the developed software are described.

[3] https://naif.jpl.nasa.gov/

Note that, in this study, it is assumed that communications with Earth will be performed through the Deep Space Network's (DSN) ground stations [26]. The DSN is operated and managed by NASA and it is a high-performance communication network capable of 24/7 communication with different deep space missions. Its coverage is ensured by the strategical locations of its three facilities at Canberra (AU), Madrid (ES) and Goldstone (USA), which, in turn, are constituted by a set of 70-m – one per station – and 34-m antennas that communicate with most of the currently operational deep space missions. Table 1 presents the list of DSN antennas considered in the software.

2.1. The contact plan

One can obtain the time period(s) where two nodes may communicate by analyzing the interval(s) where those cannot and find the complementary time periods.

Defining ψ as the logical parameter that indicates whether the communication is possible ($\psi = 1$) or not ($\psi = 0$) considering a particular hindering phenomena at a specific moment, the visibility ξ between two nodes at each time step is obtained as

$$\xi(t) = \prod_{i=0}^{N} \psi_i(t), \tag{1}$$

where i corresponds to the different evaluations of the phenomena explained hereafter.

Those aforementioned situations where two nodes might not be able to *properly* communicate are:

- Occultations
- Solar conjunctions.

The former concerns itself with the physical interruption of the communication caused by the passage of a third body between the two communicating nodes whilst the latter considers the deterioration or interruption of the communication caused by the Sun, as introduced in Section 1. There are two geometric situations where the Sun worsens the communication: the superior and the inferior solar conjunctions. The first one implies that the Sun is between both communicating nodes, not necessarily physically intercepting its line of sight, but deteriorating the communication between them due to different phenomena (intensity scintillation, phase scintillation and spectral broadening) caused by its corona, besides the thermal noise [27]. The second one involves the geometric situation where the three bodies are aligned, the Sun is at one end and Earth is in the middle. In that case, the physical link does not traverse the Sun or the solar corona, but could still be affected by the thermal noise coming from it if the receiver antenna is pointing in the direction towards the Sun – i.e., the uplink in the case of Earth–Mars communications – [5]. Superior conjunctions are substantially more critical than inferior solar conjunctions [4] as those complicate the downlink (in addition to uplink) of mission data, leading to more dramatic actions during communication windows.

Speaking in terms of the developed software, occultations, on the one hand, are calculated differently depending on the case or, more specifically, the occulting body.

As stated before, SPICE features some modules to compute specific geometric events, as is the case of the occultations. This function is suitable for occulting bodies that do not have any of the involved communicating nodes located on their surface. Provided a certain time interval, the occultations module can return the time windows where, for instance, Mars is occulting the MAVEN orbiter [28] as seen from Earth. As a matter of fact, the Contact Plan identifies, for each pair of nodes, all the relevant celestial bodies that may potentially block the communication (i.e., planets and/or satellites).

Nonetheless, when it comes to analyzing the sight line with a lander or a ground station, a different method is used to compute the aforementioned time windows. In this second case, the SPICE module that allows to compute the elevation angle of the target as seen from the observer – the one that is located on the surface of the third body – is used. Noticeably, the minimum elevation angle that ensures an effective communication depends on the third body's features. According to [26], the minimum elevation angle at which the DSN antennas may communicate is 10° (uplink) and 6° (downlink). This way one can obtain the time windows where, for instance, a DSN antenna (observer) is able to communicate with MAVEN (target).

Notice that both computations are not exclusive. For instance, if the communication involves a Martian orbiter and a DSN ground station, the final communication windows will come from the intersection of both the elevation angle approach and the occultation module outcomes.

On the other hand, the computation of the solar conjunction period consists of an evaluation of the SEP angle – through an analysis of the geometric positions of the bodies obtained from SPICE – at each time step: whenever this reaches a certain value, a solar conjunction starts, which entails that, from that point on (as the angle becomes progressively smaller), the available bit rate will progressively decrease as interference grows. However, the definition of the threshold value is not trivial; neither is the determination of the bit rate according to the solar interference level.

Some researchers have delved into the solar interference effects on deep space communications at different frequencies, procuring models that can predict the magnitude of the phenomena occurring during solar conjunctions in periods of quiescent activity and determining strategies in order to widen the communication windows in such periods, both in maximum and minimum solar activity [5,27]. In this same line, Baldi et al. [29] propose strengthening the link against the phenomenon of scintillation – appearing during the crossing of the solar corona – by using error-correcting codes and specific demodulation techniques. Yet, the current strategy during a superior solar conjunction is to subsequently scale bit rate down – according to previous experience – as the SEP angle becomes progressively smaller.[4] Acknowledging that the implementation of solar interference models remains out of the scope of this study, the present model does not consider communication during solar conjunctions.

Even so, the issue of establishing a threshold value remains. According to Morabito and Hastrup [5], during periods of normal (quiescent) solar activity, the communication between Earth and Mars becomes significantly harder at SEP angles below 2.3° in X-band and 1° in Ka-band; hence these are the threshold values that are going to limit the solar conjunction periods in the present link transfer model.

2.2. The link performance

Provided the feasibility of the communication at each time step, the link performance problem determines the maximum allowable bit rate at which two nodes can communicate.

Broadly speaking, bit rate is related to bandwidth – which is, in turn, determined by the communication system's modulation – and the Signal-to-Noise ratio, explained hereafter. The quotient between the received signal power and the noise power, otherwise known as the Signal-to-Noise ratio, is

$$SNR = \frac{P_t\, G_t\, G_r}{L\, B\, k_B\, T_{sys}}, \tag{2}$$

where P_t is the transmitted power in W, G_t and G_r are the transmitter and receiver antenna's gain, respectively, L is the product of the free-space path, antennas' hardware, polarization and pointing losses, B is the channel bandwidth in Hz, k_B is the Boltzmann constant and T_{sys} is the system equivalent noise temperature in K.

From the statement above, one can deduce that the minimum admissible SNR considers the maximum needed bandwidth at which two nodes may communicate, which, in turn, dictates the maximum allowable symbol rate S depending on the modulation system employed.

Provided the bandwidth, in general,[5] it is given [30]

$$S = B. \tag{3}$$

Likewise, the relation between symbol rate and bit rate depends on the communication system's modulation method. For instance, MRO communications may apply Quadrature Phase-Shift Keying (QPSK) [6], which can forward at a bit rate R

$$R = 2 \cdot S. \tag{4}$$

Although different modulation methods have been applied throughout the lifetime of MRO [6], this study implements QPSK for all communication links (including MRO's). Notice that the usage of turbocodes or convolutional codes that may improve link performance (lower SNR_{min} or higher bit rates) [30] are not considered in this analysis.

Thus, to recap, the successive bit rates at which MRO may communicate with Earth can be computed as follows

$$B_{max} = \frac{P_t\, G_t\, G_r}{L\; SNR_{min}\, k_B\, T_{sys}} \xrightarrow{\text{QPSK}} R_{max} = 2 \cdot B_{max}. \tag{5}$$

However, DSN communications are restricted by their own channel allocations. Namely, each mission is assigned a DSN channel, which sets

[4] Personal communication with Jim Taylor.

[5] It depends on the pulse shape. The equation expresses the maximum practicable symbol rate.

a frequency for communications and a maximum bandwidth B_{channel}. Therefore, $B_{\max}$ cannot exceed the latter value, which ultimately limits the maximum communication bit rate with the DSN ground stations within the stated channel. Using the previous MRO case study, the latter means

$$\text{if} \quad B_{\max} > B_{\text{channel}}, \quad \text{then} \quad R_{\max} = 2 \cdot B_{\text{channel}}. \tag{6}$$

There is still one parameter left to determine: the $SNR_{\min}$, which is related to the receiver telecommunication system as follows

$$SNR_{\min} = \frac{P_s}{Bk_B T_{\text{sys}}}, \tag{7}$$

where P_s corresponds to the receiver sensitivity, i.e., the minimum received signal power at the receiver input so the signal does not get embedded in the system's noise. In the absence of the DSN receiver's sensitivities, $SNR_{\min}$ was obtained through the mining of DSN-MRO communications data – the selected study case – explained in Section 2.4. For all other cases, it has been assumed $SNR_{\min} = 10$ dB.

All of the variables needed to compute the maximum bandwidth – except for the minimum acceptable Signal-to-Noise ratio and the Boltzmann constant – are intrinsic to the telecommunication system design, i.e., the antennas, the frequency of communication, the modulation system, the electronic components, etc. Therefore, to accurately compute the capacity of a certain link, the corresponding parameters have been obtained from the respective telecommunication system design handbooks [6,26]. In the case of the DSN antennas, some of these parameters are calculated by means of models, such as the antenna's gain, which is dependent on the elevation angle at which the antenna is pointing[6] [26]; some others, such as the system noise temperature or the atmospheric attenuation, are dependent on the scenario, i.e., the specific antenna's configuration or the atmospheric conditions, respectively. In the latter cases, the most restrictive values – i.e., the worst case scenarios – have been chosen in order to provide with a lower bit rate boundary.

The relays, conversely, need to be designed from scratch. As a starting point in this study, their telecommunication system is going to be based on the third-generation Tracking and Data Relay Satellites (TDRS) [31]: a 10-satellite geosynchronous constellation devoted to providing near-continuous communication support to different missions, such as the ISS [32]. This way, the implementation of the new network topologies employs currently-available technologies. Although it seems reasonable to assume more advanced capabilities for the relays – as these are envisaged in a futuristic scenario –, this study intends to, firstly, analyze the present capabilities. Later on, an analysis on capacity evolution with improved relay designs is also presented and discussed. Finally, since all the involved communications are digital, the relays are assumed to be regenerative [13,33]. This is, before the relay hands over the information to the next communicating node, the signal goes through a process of amplification, demodulation, decodification, error detection and correction (EDAC) before encoding, modulating and transmitting it again.

As these parameters are intrinsic to the telecommunication system, the software includes a database that retrieves all of these variables (at each time step if these are time-dependent) subject to the communicating node involved, i.e., specific spacecraft, DSN antenna and/or relay.

As stated earlier, the communication frequency with a DSN antenna is already determined by the DSN channel allocations [26]. However, the communication frequency of the links that do not involve any of the DSN antennas is not determined, therefore constitutes a design parameter, and hence it has been optimized. This is, for this specific scenario – i.e., Earth–Mars communications –, and since the distances are relatively small, it has been obtained that the Ka-band (∼ 32 GHz) provides with better results than the X-band (∼ 8 GHz) as both gain and space losses depend on the wavelength. For future works, notice that this might not be the case for other case studies where longer distances are considered, as the enhancements (antenna gain) that come with the Ka-band might not overcome the increase in space loss as compared to the X-band.

2.3. The routing algorithm

On the whole, the contact plan and link performance models enable a quantification of the transmission rate at which two nodes may communicate, wherever possible. Abstracting this to the broader picture, those ultimately allow to build a map of the different transfer rates between all of the available communicating nodes (orbiters, relays, ground stations, etc.) at each time step within a specific time period. In other words, the software successively builds a graph where the vertices are all of the active antennas and the costs (edges) between them are a value proportional to the bit rate. In this scenario, the routing algorithm finds the optimal path that goes from the source to the destination at all times.

Notice that each two-node link is acknowledged as hop or contact; therefore, the one-hop (or direct) link entails a single contact, the two-hop link involves two contacts, and so on. The resulting path contains the different hops that a communication goes through to deliver a message from the sender to the receiver.

The optimization criteria is the equivalent bit rate of the path, which can be computed in two different ways considering the relay design:

- On the one hand, the relay may carry two High Gain Antennas (HGA), hence it can deliver the information as it is received. This is acknowledged as simultaneous communication, and the equivalent bit rate is computed as

$$R_T = \min\{R_i\}, \quad i = 1, 2, \dots, M, \tag{8}$$

  where M is the number of hops in the route.
- On the other hand, the relay may carry only one HGA, thus it cannot return the message until forwarding has ended. This is acknowledged as consecutive communication. Notice that, in this case, the time that the antenna takes to go from one pointing profile to the other, in order to align itself with the target, is not taken into account. In a system of N communication nodes with a single antenna, the total time for the information transmission is

$$\Delta t = \sum_{i=1}^{N} \Delta t_i, \tag{9}$$

  where

$$\Delta t_i = \frac{D}{R_i}, \tag{10}$$

  being D the data volume and R_i the transmission bit rate of the ith node. Then,

$$\Delta t = \frac{D}{R_1} + \frac{D}{R_2} + \cdots + \frac{D}{R_N} = D\left(\frac{1}{R_1} + \frac{1}{R_2} + \cdots + \frac{1}{R_N}\right). \tag{11}$$

  Thus, the equivalent bit rate is computed as [34]

$$\frac{1}{R_T} = \sum_{i=1}^{N} \frac{1}{R_i}. \tag{12}$$

These two communication strategies lead to different search algorithms. Albeit algorithmically similar, the first one finds the path with the maximum bottleneck – Widest Path Problem – whereas the second one returns the path with the minimum total cost – Shortest Path Problem – (notice from the consecutive approach stated above

[6] This is due to the structural deformation of the antenna when it is pointing at an elevation angle other than the angle where the reflector panels were aligned.

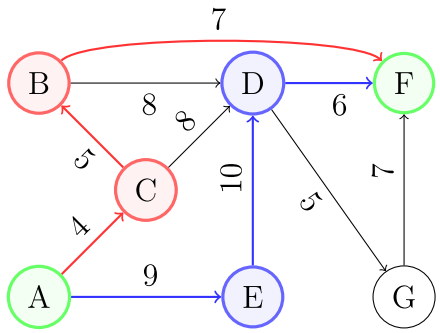

Fig. 2. Graph example. The blue nodes and arrows denote the optimal path from A (source) to F (destination) obtained with the Widest Path algorithm. The red ones correspond to the analogous case study with the Dijkstra algorithm. The weights in the graph – i.e., the cost between two vertices – correspond to $1/R_i$ (Dijkstra) or R_i (modified Dijkstra). (For interpretation of the references to color in this figure legend, the reader is referred to the web version of this article.)

that the minimum total cost leads to the maximum equivalent bit rate), as seen in Fig. 2. Thus, for consecutive communication we implement the Dijkstra algorithm [35], whilst simultaneous communication uses a modified version of the former. It is worth mentioning that these search algorithms do not consider the time the antenna takes to change its aim from communication node to the other.

Moreover, it is possible to evaluate scenarios with more than one source and/or destination nodes, where additional vertices – acknowledged here as fictitious nodes – are enabled. For instance, if one wants to analyze the evolution of the communications between a Martian orbiter and Earth – regardless of the facility –, the software allows to choose EARTH-34 or EARTH-70, which would integrate the three 34-m or 70-m DSN antennas, respectively. The fictitious nodes can only communicate with the group of nodes they represent and at an infinite rate. This way, the routing algorithm warrants choosing the most suitable DSN antenna to communicate with the orbiter at each point in time.

2.4. DSN data mining

This study also includes an analysis of the DSN communications through its public online database where one can access all the communication data from the last 6-years.[7] This data mining has been performed for two reasons:

1. To validate the Contact Plan.
2. To obtain the SNR_{min} parameter for the DSN antennas.

Thus, all the data collected from 2013 to 2019 – sampled every 5 seconds – have been processed and used to perform the aforementioned analysis. In order to validate the data mining itself and its subsequent post-processing, the bit rate evolution of the Rosetta mission on the final stage of its service life presented in [36] is used as a baseline to compare against the bit rate evolution obtained through the processing of the DSN data. Results are presented in Fig. 3. Despite minor differences, it can be inferred that the DSN data have been correctly processed, both for the 34-m and the 70-m antennas.

Regarding the contact plan's validation, it is known that the DSN owns its particular communications schedule with the different spacecraft, which means that validation procedures should be encompassed within the predicted visibility computed by the contact plan. Indeed, compliance with the predicted visibility time windows with the actual DSN schedule (DSS-65 and DSS-24 antennas, respectively) for the Juno and MRO orbiters, at different time periods, is shown in Fig. 4. As explained in Section 2.1, visibility is a binary parameter, where a value of 1 means communication is feasible and a value of 0 that it is not.

Finally, the Direct-to-Earth bit rate of the MRO spacecraft with the DSS-45 antenna from 2014 to 2016, obtained through the Link Transfer Model and the DSN mined data, respectively, are presented in Fig. 5. The figure also displays the Earth–Mars distance over time (green line). Note that both bit rate evolutions are quite similar except for the time period between January 1st, 2014 to July 15th, 2014, where the predicted bit rate is significantly higher (up to 2 times) than the one used (3 Mbps). The reason is that downlink rates can vary according to the needs of the mission, and are not necessarily chosen on the basis of maximizing the bit rate.[8] Therefore, during the time period where Earth and Mars distance is at its lowest, MRO may not need to take up all the available bit rate and simply communicates at a reasonable speed. At other times, however, it is assumed that MRO indeed communicates at its maximum speed, and that is the hypothesis from which the SNR_{min} parameter presented in Section 2.2 is obtained. Namely, Eq. (5) defined the relationship between the bit rate and the maximum bandwidth, which is in turn computed through the respective telecommunication parameters. In the DSN case, all of the aforementioned telecommunications variables were retrieved from [26], except for SNR_{min}. Therefore, the latter has been inferred from the actual MRO-DSN downlink bit rate for each of the antennas; Fig. 5 shows the results for the DSS-45 antenna case.

3. Network topology

Two different network structures are proposed and assessed here. The first topology consists of the location of relay satellites at the Earth–Sun system Lagrange points L_3, L_4 and L_5 whilst the second one relates to the location of an N-constellation of relay satellites in a heliocentric circular orbit between Earth and Mars.

Hereafter, a description of both approaches is presented as well as their main differences and underlying rationale.

3.1. The Lagrange-relays network topology

The Lagrange points are the 5 stationary locations of a body's orbital motion subjected to the gravitational forces exerted by two larger bodies –i.e., Earth and the Sun in our case. These stationary solutions are a product of the balance between the gravitational and the centripetal forces, hence when the body – e.g., a probe – is located at one of these libration points, it remains fixed at that position in a co-rotating frame of reference in which the two larger masses hold fixed positions (the Synodical Barycentric Reference Frame).

As a matter of fact, the stability of these stationary solutions is important as it dictates the station-keeping costs of the probe's orbit. Dynamically unstable points, such as L_1, L_2 and L_3, cause the probe to drift away from those positions, provided any small perturbation. Yet, the L_3 libration point is much less unstable than the other two. Conversely, in the Earth–Sun system, L_4 and L_5 are dynamically stable points, which induce the probe to describe a stable orbit around those, given any perturbation.

In this study, the Earth–Sun system libration points L_3, L_4 and L_5 were chosen to constitute a network topology that may relay communications with Mars. The remaining two Lagrange points were dismissed due to their close proximity with Earth, which would not make any difference in terms of distance to Mars (space loss) and, besides, the relay's capabilities in terms of telecommunications system are inferior than the DSN stations', thus the latter would always provide better performance.

[7] https://eyes.nasa.gov/dsn/data

[8] Personal communication with Jim Taylor.

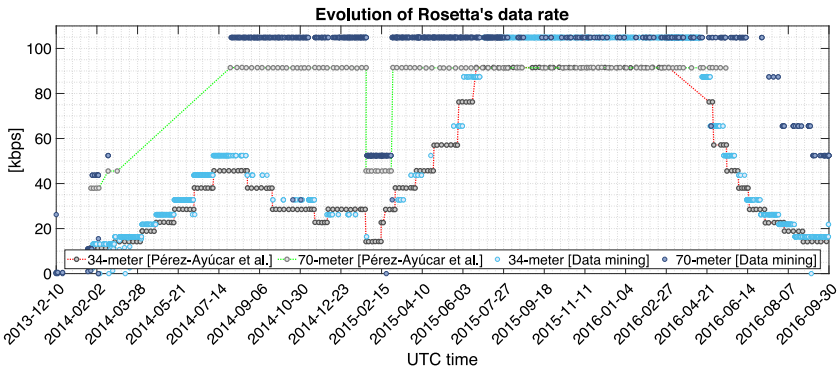

Fig. 3. Comparison of Rosetta's bit rate evolution between the data mined from the DSN and the data obtained from [36].

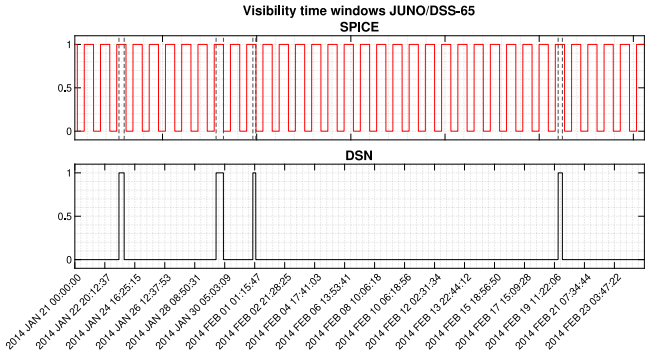

(a) Juno

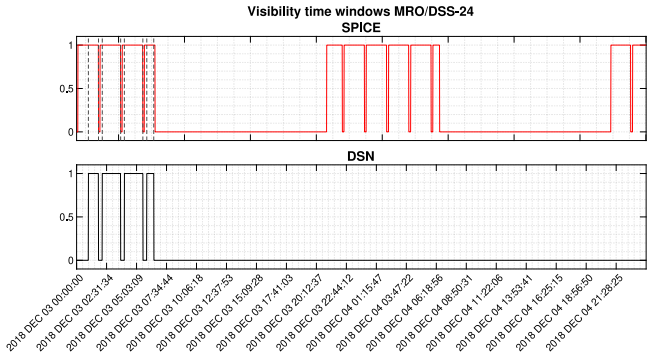

(b) MRO

Fig. 4. Comparison of DSN's actual communication windows (bottom) and the time windows predicted by the contact plan (top).

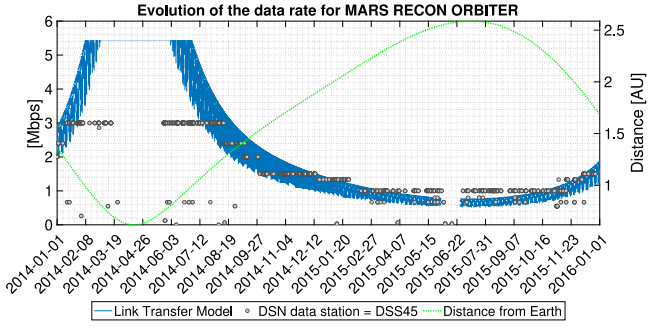

Fig. 5. Bit rate evolution between MRO and DSS-45 antenna. The blue line shows the predicted maximum bit rate through the Link Transfer Model. The gray dots correspond to the actual used bit rate, obtained through the DSN data mining. (For interpretation of the references to color in this figure legend, the reader is referred to the web version of this article.)

Since the Lagrange points are always at the same relative position with respect to Earth, the bit rate between the L_4/L_5 relays and the Earth is always the same, except for the elevation angle effects, which affects the DSN antennas' gain (see Section 2.2). The L_3 libration point, for its part, is always facing the opposite side of the Sun as seen from Earth, making it unable to directly communicate with the latter but very appealing to relay communications with Mars during a superior conjunction, supported by the L_4/L_5 relays.

Moreover, another benefit emerges from this approach: an increase in communication availability. As stated in Section 1, the DSN is able to provide 24/7 coverage through its strategically located stations, provided there is a usable line of sight. Still, once a spacecraft sinks into the horizon as seen from a specific antenna, the former will remain unreachable for several hours until it rises again over the horizon. The same applies to surface spacecraft such as rovers, although their communications with Earth are usually relayed by orbiters (higher capacity). On the other side, orbiters are also subject to occultations by Mars. This means that, all things considered, visibility between Martian missions and ground stations is consecutively subject to occultations of both Mars and Earth –i.e., their respective centers of motion.

In contrast, with the incorporation of Lagrange relays, the number of link supports increases and, although Mars and Earth will continue to interfere, the communication route is split into different hops, therefore the end-to-end path can find alternative options, even with less DSN antennas, as will be seen in results.

3.2. The pearl constellation topology

Unlike the former configuration, the pearl constellation presents two design degrees of freedom that shall be determined: the number of satellites N – a design variable – and the radius of the orbit R_N – an optimizable variable –, assuming the latter is circular.

As a first attempt in this study, two configurations are going to be studied: $N = 3$ and $N = 4$. The first one allows for direct comparison with the Lagrange-relays network topology with an optimized orbit. The second one, as it increases the number of relays by 1, enables to analyze the impact on the mean bit rate as well as the communication availability when compared to the other two, all the while preserving a reasonable number of satellites to be placed in orbit. In Section 4, the effect of the number of satellites on the bit rate evolution will be further discussed. Noticeably, the optimal R_N is the one that provides the greatest bit rate –calculated in both the simultaneous and consecutive scenarios. To do so, the time evolution of both bit rates is analyzed for different R_N values over a long period of time, for the pearl constellation with 4 satellites. This large period of time corresponds to the three-body "synodic" period of the Earth, Mars and the constellation of

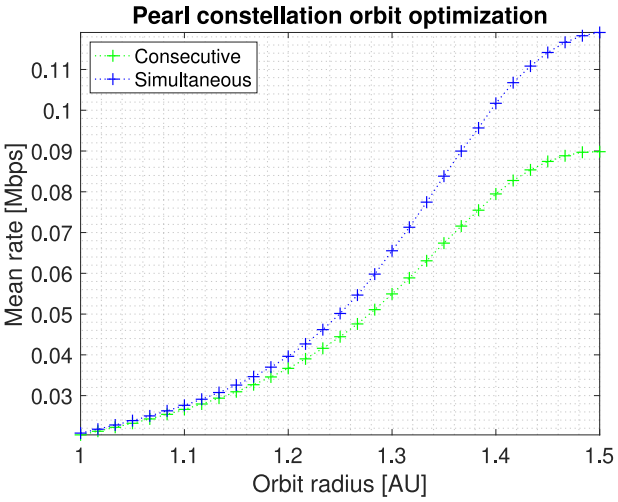

Fig. 6. Pearl constellation orbit optimization with $N = 4$.

relays, which is equal to the time it takes for the three bodies to be in the same configuration they started with at $t = 0$.[9]

It should be noted that the bit rate evolution during this time interval could be embodied by the minimum, peak or average values of the whole progression, however the first one is not meaningful because it could be avoided with other, alternative routes, whilst the second one may become misleading as its evolution fluctuates highly over the whole time period due to the quadratic evolution of the bit rate with the inverse of the distance (space loss). More specifically, there are points in time where the distance between the three bodies is significant and exceptionally reduced, which leads to a dramatic increase of the bit rate as compared to other peak values over the time interval. Thereupon, the bit rate over the three-body "synodic" period is going to be represented by its mean value at each orbit size iteration.

The outcome of the aforementioned analysis is shown in Fig. 6. As can be seen, the optimal radius is the one closest to Mars, and, as a matter of fact, this already reveals that the link between the spacecraft and the first –closest– relay always constitutes the bottleneck within the overall path. Noticeably, this conclusion may be abstracted to the pearl constellation with 3 satellites, whose evolution would also be constrained by the aforementioned bottleneck link. The 3-satellites mean bit rate evolution with orbit radius would be akin to the 4-satellites one, only with lower magnitudes of the first due to the lesser number of satellites. Therefore, the optimal radius for both constellations is going to be the same. This is further discussed in Section 4, as is the trend of the optimal R_N with the relay capabilities' enhancements. In order to avoid Mars' orbit, the pearl constellation orbit size at its current design is $R_N = 1.4$ AU.

Although the pearl constellation orbit might be more unstable than the Lagrange points, it provides higher bit rates than the former as the relay locations are optimized according to the bit rate needs. Yet, the stability of the orbit remains as a qualitative variable in this study, even if it is critical to decide the suitability of the approach until a quantitative assessment is performed (out of scope). Finally, and analogously to the former topology, this network also guarantees increased communication availability.

[9] For the calculation of the three-body synodic period, some margin for the angle formed by the three bodies has been given; otherwise, finding a perfect alignment (i.e. the angle is equal to 0) would result in a very long period.

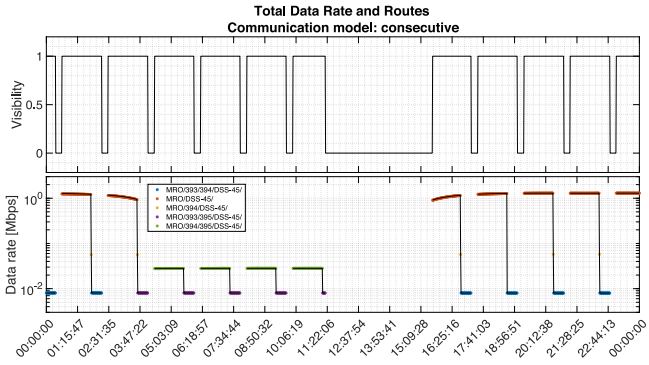

Fig. 7. Top: visibility time windows between MRO and DSS-45 throughout January 20th, 2018, when the Lagrange-relays network topology is enabled. If the communication is possible, the visibility value is equal to 1. Bottom: bit rate evolution. The black line follows the communication, i.e., when the latter is interrupted (no visibility), so is the line. (For interpretation of the references to color in this figure legend, the reader is referred to the web version of this article.)

Table 2
Summary of IDs used to designate the different communication nodes.

ID	Description
MRO	Mars Reconnaissance Orbiter
DSS-45, DSS-15, DSS-65	DSN 34 m antennas
L_3, L_4, L_5	Earth–Mars system L_3, L_4 and L_5 libration points, respectively
R_1, R_2, R_3, R_4	Pearl constellation nodes
EARTH-34	Earth fictitious node that enables the communication with any of the DSN 34 m antennas

4. Results and discussion

Before a presentation and discussion of results is introduced, a short schematic of the case studies and scenarios will be explained in the next few lines. First of all, recall that the DSN owns two different kind of antennas: 34-m and 70-m antennas, from which only the former are considered here. Furthermore, two possible combinations of antennas are analyzed: one where all three 34-m antennas – from the three different stations – are available and another where only one antenna is accessible. Second, there are two communication strategies considered in this study: simultaneous and consecutive models (see Section 2), which will lead to different path-equivalent bit rates. Third, there are two network topologies: the Lagrange-relays and the pearl constellation topologies (see Section 3). Fourth, in all cases, the Martian spacecraft has been arbitrarily chosen to be the Mars Reconnaissance Orbiter (MRO) [6] and the designed relay capabilities are equal to that of the TDRSS for the first analysis. Fifth, the respective communication frequencies are, on the one side, the ones designated by the DSN channel allocations (X-band) for communications with Earth and, on the other side, the Ka frequency band for any other type of communication link (see Section 2.2). Sixth, all communication node designations correspond to their NAIF ID names [37], except for the pearl constellation and the Earth–Sun system Lagrange point L_3, whose kernels have been built from scratch and so have their IDs. A summary of the IDs used for the different communication nodes is presented in Table 2. Finally, the following outcomes are evaluated during a time period of 2 years, the synodic period of Mars (approximately), arbitrarily chosen to be the time window that goes from 2017 to 2019. It is important to note that any other time period would involve changes to all of the numeric results presented hereunder, as discussed later.

In order to ease the comprehensibility of the subsequent results, Fig. 7 shows the bit rate evolution of MRO communications with a single DSN antenna (DSS-45) over the course of a day. In this case,

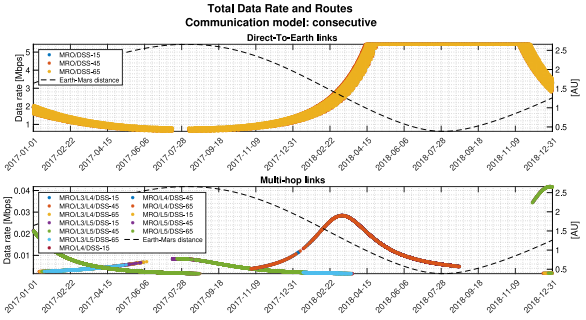

Fig. 8. Bit rate evolution of MRO communications with Earth's 34-m DSN antennas when the Lagrange-relays network topology is enabled (consecutive model). Top: DTE communications. Bottom: communications via Lagrange relays. In addition, the figures also include the Earth–Mars distance evolution (dotted black line, referred to right y-axis). (For interpretation of the references to color in this figure legend, the reader is referred to the web version of this article.)

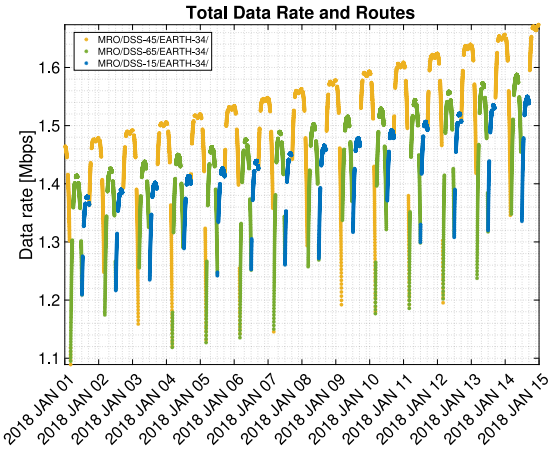

Fig. 9. Cascading effect caused by the DSN antenna alignment.

the Lagrange-relays network topology is enabled. The figure at the bottom shows the bit rate, at each time step, selected by the routing algorithm as the optimal one for each possible link. The corresponding routes are captioned within the legend. As a matter of fact, the graph also displays the total visibility time windows of such communication (top figure) for two reasons. The first one is to show the nature and impact of the occultations to which Earth–Mars communications are normally subjected to.[10] In the visibility evolution, longer gaps of the communication are associated to the DSN, i.e., the DSN antenna is not accessible (due to physical occultation of Earth or because the elevation angle of the spacecraft as seen from the antenna is too small). Shorter gaps are associated to MRO, i.e., the orbiter is occulted by Mars. The second reason is to show the consecutivity of the communication (as well as the gaps) when the relays are displayed. The bit rate evolution shows how the network topology enables a greater number of link supports that may sustain the communication when the DTE link is not available, as discussed hereafter.

Continuing with the entire simulation over the Martian synodic period, Fig. 8 shows the bit rate evolution of the communication between MRO and the DSN when the Lagrange-relays network topology –with a consecutive model of communication– is enabled, along with Earth–Mars distance. For the sake of comprehensibility, the end-to-end bit rate progressions have been split in two – the DTE link at the top and the multi-hop links at the bottom – even though all the communication paths are consecutive in time – there are no two simultaneous points between the different evolutions. Since all three 34-m antennas are accessible, as well as all three Lagrange relays, the number of possible node-to-node links is quite significant and therefore routes are diverse, as can be seen in the legend. Those evolutions with the best performance correspond to the DTE links, whilst the lower bit rates are associated to the communications via relay. Moreover, when focusing on the top performing links, a cascading effect can be appreciated, illustrated in Fig. 9, caused by the evolution of the antenna's gain with the elevation angle of the spacecraft as seen from the station over time [26].

Notice that the analogous results of Fig. 8 with only one DSN antenna are not shown because the main difference with the former lies within the availability, which would not be visible in the results due to the high number of values.

It is quite noticeable that the DTE link bit rate is significantly better – up to 2 orders of magnitude – than that of the communication via relay. This is due to the spacecraft-relay link, which introduces a major bottleneck as a result of the relay's capabilities, as it cannot surpass the performance of DSN receivers and large antennas even at a close distance to the spacecraft (lesser space loss). Consequently, the Lagrange-relays network topology at present would be relegated to those situations where MRO and the DSN stations cannot communicate due to occultations (see Fig. 7). However, there is one noticeable point of interest in this network topology: communication availability, especially during solar conjunctions. Indeed, and as already explained in Section 2, during superior solar conjunctions, the Sun is causing significant interference, which, combined with the achieved Earth–Mars peak distance, lead to a dramatic drop of the bit rate, in some cases down to zero values [7]. The Lagrange-relays topology, however, enables real-time communication by means of combining L_3 with L_4/L_5, successfully avoiding the superior conjunction.

Table 3
Communication availability over a two-year period. The left column corresponds to the Direct-to-Earth link, the middle and right columns encompass all the possible combinations of links when the Lagrange-relays and the pearl constellation network topologies are enabled, respectively. Notice that the DTE link is also considered in both network topologies cases.

DSN stations	DTE link	Lagrange	Pearl N = 3	Pearl N = 4
1	34 %	77 %	91 %	98 %
3	70 %	91 %	98 %	100 %

However, the improvement on communication availability is not only relevant for solar conjunctions. Hereunder, the percentage increase of communication availability is summarized in Table 3, for both the case studies with three and one available DSN antennas. Notice that, as a matter of fact, even when the three DSN antennas are available, the DTE link may not guarantee continuous communication, as MRO gets inevitably occulted by Mars during a short period of time of its orbit around the planet, which amounts to almost 30% of the time when integrated over the 2-years synodic period. Nevertheless, the Lagrange-relays network may provide with similar – in fact, slightly higher – communication availability with only one DSN antenna, and up to 91% availability when the three facilities are accessible. The one-antenna case enhancement deserves to be insisted upon as availability could be improved up to 43%. On the one hand, this certainly strengthens the robustness of the overall deep space communications network, as this result is showing that, in case any two of the three DSN facilities are inaccessible, only one antenna could cover as much as all three currently do – see the percentage availability of the DTE link of all three antennas – for this mission. On the other hand, this could ease deep space communications for local, single ground stations other than the DSN.

[10] Except when solar conjunctions occur.

Moving forward to the next configuration, Fig. 10 presents the evolution of the bit rate values for the 3- and 4-satellites pearl constellations over time, analogously to the Lagrange-relays topology's progression. When compared to the latter, although better bit rate values can be noted due to orbit size optimization in this case, the shorter distance between the spacecraft and the relay still cannot make up for the relay's telecommunications system limitations. Likewise, the DTE link surpasses the multi-hop link values at all times.

It is worth mentioning that the pearl constellation with 3 satellites shows a better performance than the one with 4 satellites. For a certain amount of time, the former topology becomes even comparable to the DTE link. This difference in performance between the pearl constellation topologies is correlated to the three-body "synodic" period between the bodies, i.e., the time it takes for Mars and the constellation of relays – regarded here as a body itself since their relative position is fixed – to be at the same angular position with respect to Earth. This period is considerably higher than the 2-years Martian synodic period. In consequence, the outcome of Fig. 10 only contains a part of all the possible geometric positions between the bodies, which ultimately results in different link performance over the same time period, as discussed later.

On the other hand, going back to Table 3, the availability results show that, for the single DSN antenna case, the pearl constellation with 3 satellites increases the availability by a 57% with respect to the direct link. Thus, just by changing the relays orbit the availability is 14% better than the former topology. As a matter of fact, this value is very close to the one with one additional relay, which raises the availability increment up to 64%. With all the ground stations facilities enabled, the spacecraft may communicate almost – 3 satellites – or completely – 4 satellites – 100% of the time. Overall, the same conclusions inferred for the Lagrange-relays case study are still valid (with even better performance) for the pearl constellation case, but enabling continuous communications is a major improvement with respect to the oncoming crewed missions, as communications are very critical for their success.

As stated at the beginning of this section, it is acknowledged that any other synodic time period could have led to different results. The reason is that the relative geometry between the communication nodes may change over a time span – the three-body "synodic" period – larger than the Martian synodic period. This time period contains all the possible relative positions between the bodies. Thus, to be able to evaluate the complete progression of all the possible communications (two-node links) involved in the network topology, one would need to simulate the configuration over the aforementioned time interval. However, its value is considerably high and, therefore, for the sake of simplicity and preserving a good readability of the results, it is chosen to analyze the evolution of the different links – separately – over a 15-years period, which corresponds to the Earth–Mars inertial repeat period. These progressions can be seen in Fig. 11 for the three different network topologies, respectively, along with the evolution of Earth–Mars distance. On the whole, there are four identifiable types of links involved in any of the network topologies: (1) the link between the spacecraft to any of the intermediate relays, (2) the link between relays, (3) the link between the relays and Earth's ground stations and (4) the Direct-To-Earth link, which provides a reference to determine the quality of the other links. Starting from the Lagrange-relays topology, Fig. 11 shows that the link between the spacecraft and the relay is a bottleneck. Thus, shortening the distance between them would improve – quadratically – its performance. The pearl constellation topology arises from this realization. Taking a look at the pearl constellation evolutions, the aforementioned link indeed increases, although it is still insufficient when compared to the DTE link — altogether, the pearl constellation topologies still show a very limited outcome. It is worth mentioning that the pearl constellation with 3 satellites shows a better performance than the one with 4 satellites over the 15 years, in an equivalent manner to Fig. 10. As stated before, this is due to the three-body "synodic" period, as the Earth–Mars inertia repeat

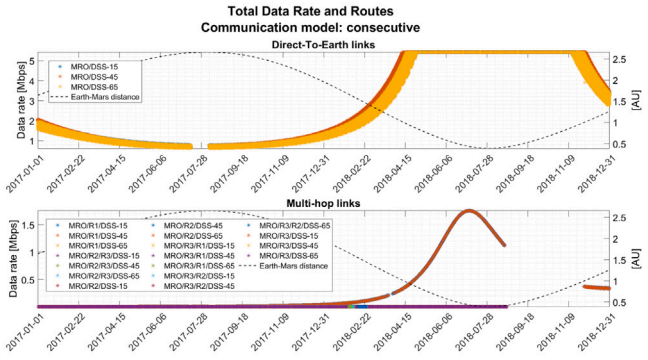

(a) Pearl constellation N=3

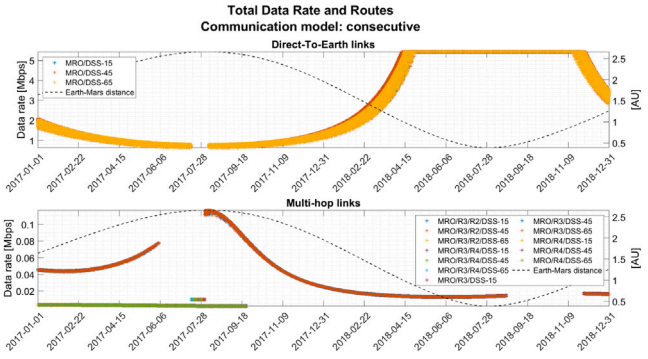

(b) Pearl constellation N=4

Fig. 10. Bit rate evolution of MRO communications with Earth's 34-m DSN antennas when the 3- and 4-satellites pearl constellations are enabled (consecutive model). Top: DTE communications. Bottom: communications via pearl constellation. In addition, the figures also include the Earth–Mars distance evolution (dotted black line, referred to right y-axis). (For interpretation of the references to color in this figure legend, the reader is referred to the web version of this article.)

period only shows a part of all the possible arrangements between the communication nodes, which has two implications. On the one hand, if the simulation time period had been extended (three-body "synodic" period), the 4-satellites configuration would eventually match those peaks seen at the 3-satellites pearl topology. On the other hand, it may take over, at least, 15 years to reach a geometry that leads to this performance scenario.

Another aspect worth considering is that the size of the pearl constellation orbit – as compared to the Lagrange network topology – reduces significantly the peak performance frequency of the spacecraft-relay link. In other words, taking a look at the pearl constellation evolution with three satellites, the close encounters – higher link performance – between the spacecraft and each of the relays occur very separately on time, leaving long time windows where the satellites are far away from Mars and, thus, the multi-hop link is largely constrained. Therefore, the pearl constellation with 4 satellites is deemed more adequate in overall performance than the one with 3 satellites. Hence, for the second part of this study, only the pearl constellation with 4 satellites is going to be analyzed.

Accordingly, two main conclusions can be inferred up to this point: the strategic location of relays in space is quite appealing from the availability point of view, but the usage of state-of-the-art technology is not practicable, as the obtained rate values cannot compete with the DSN antennas. As explained in Section 1, bit rate is fundamental for the potential enhancements of the DSN, as it allows to improve the efficiency of the communication (less time or higher data volume). This bit rate is strongly affected by two main features of deep space communications:

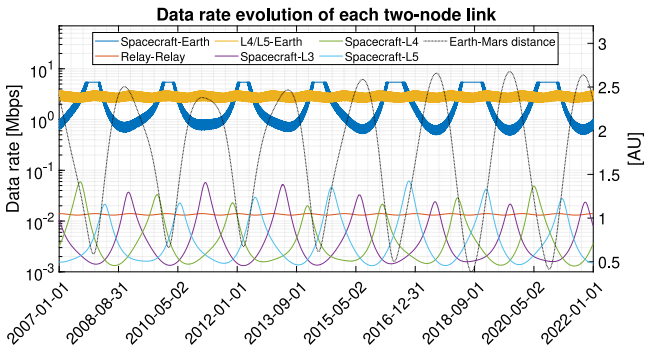

(a) Lagrange-relays network topology

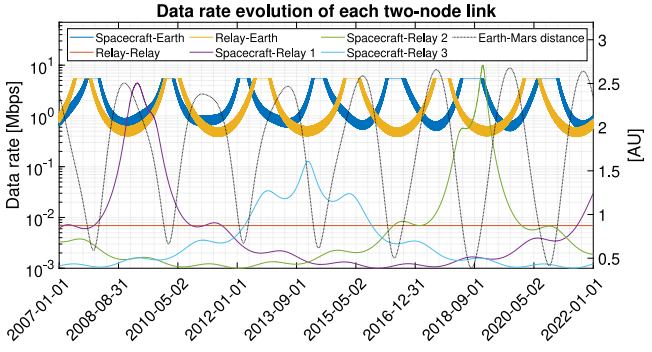

(b) Pearl constellation with 3 satellites

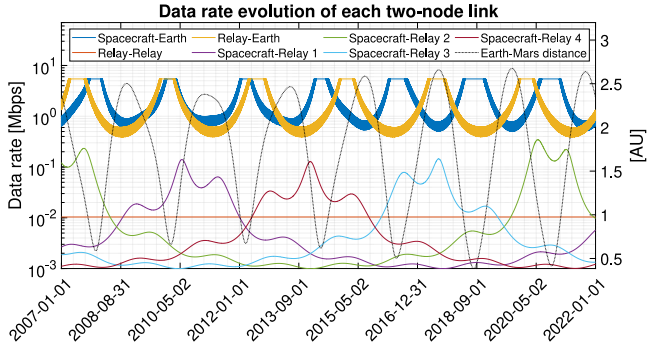

(c) Pearl constellation with 4 satellites

Fig. 11. Breakdown of each simple link evolution over a time period of 15 years for the three network topologies. In addition, the figures also include the Earth–Mars distance evolution (dotted black line, referred to right y-axis). (For interpretation of the references to color in this figure legend, the reader is referred to the web version of this article.)

- Distance
- Antennas.

Regarding distance, space losses, which increase with the squared distance between the two communicating nodes, are significantly higher than in any other type of RF communication, which severely limits the potential capacity of the link. As for antennas, their capabilities in spacecraft are essentially constrained by launch and power requirements. Namely, the gain of an antenna is proportional to its squared diameter, which is ultimately limited by volume and mass restrictions during launch. Besides, power in deep space is limited; e.g., by the size of solar power arrays – which, in turn, are again constrained by mass and volume restrictions – or the battery capacity. Consequently, the spacecraft has to accurately prioritize its limited power budget among the different subsystems. This implies that the telecommunications system gets an amount of power that is in all cases far lower than that of the DSN ground-stations. Thus, overall, deep space communications are heavily limited by gain, RF power and space losses. So far, this study has intended to address the space link issue by splitting the total link in two or more hops along the way, which reduces distance all the while improving link availability. As a matter of fact, the overall capacity for each hop –the ones that do not involve the ground stations– is not only affected by smaller space losses but also by extended bandwidths, as these need not be limited by the DSN channel allocations.

In light of this, the next step is to study what capabilities should the relay implement in order to make the overall network topology bit rates comparable to the Direct-To-Earth link. Starting with the Lagrange-relays network topology, Fig. 12 shows the evolution of minimum, maximum and average bit rate values over a two-year period versus the relay antenna's gain increase. The fundamental objective of the relay capabilities' enhancements is for bit rate to not exceed that of the direct link to Earth – in fact, the maximum cannot be exceeded due to the channel allocation restrictions of the DSN, discussed hereafter –, but that it shall be comparable and therefore complementary, especially when the DTE link is at its lowest bit rates (longer distance between Earth and Mars). Taking a closer look at the figures below, the [20, 39] dB range shows a dramatic escalation of the bit rate in all cases, narrowing down the required capabilities to this range: lower values would be insufficient and higher ones would provide poor benefits, as explained next. Noticeably, the minimum, maximum and average bit rate values eventually reach an asymptotic value that corresponds to the channel bandwidth restriction imposed by the DSN (recall Section 2.2). The relays and the DSN always communicate at this asymptotic value – even at nominal relay capabilities –, thereby one can readily identify when their link is becoming the communication bottleneck for the overall communication between Mars and Earth. Indeed, when the maximum bit rate reaches the asymptote in the simultaneous model, the link between the relay and the DSN becomes the bottleneck for some time intervals. This is also shown in Fig. 13: when the link between the spacecraft and the relays exceeds the $\sim$ 5.5 Mbps upper bound, the link between the relay and the DSN becomes the bottleneck. From that point on, the link bit rate between the spacecraft and the relay is becoming increasingly larger, whilst the link between the relay and the DSN can no longer follow this increase due to the DSN channel allocation restrictions, permanently bounding the maximum achievable bit rate to this constant value.

As a final solution, the 25 dB gain increase is chosen, as it satisfactorily meets the primary goal stated above, although this implies a significant enhancement of telecommunications hardware. In Fig. 13, the progression of each possible link over a time interval of 15 years in the Lagrange-relays network topology with a 25 dB gain increase is presented. Notice that, over the 2.1-years Martian synodic period, the links between the spacecraft and the different relays reach their respective maxima at different time intervals, as compared to the DTE link, which would only show one peak value during this time interval. Extending this analysis to the 15-years period, the peak values of the links between the spacecraft and the Lagrange relays may change due to variations between the Earth and Mars geometry, but in all cases these lie in a range of values that is at least comparable to the DTE link, if not outperforming the latter.

On the pearl constellation topology, recall that, whilst the Lagrange relays are contained within an orbit that is equal to Earth's (or similar in the case of L_3), the former is placed in an orbit that optimizes the overall bit rate of the set of relays (see Section 3). Thus, Fig. 14 presents the mean rate evolution with orbit size at different relay antenna's gain increase. This optimization has been performed within the nominal capabilities of the relay telecommunication system –i.e., state-of-the-art telecommunication system technology. Better capabilities will likely lead to other – smaller – optimal orbit size values, as shown in Fig. 14. Nevertheless, and due to the DSN channel allocation, another phenomenon overlaps: as the relay capability substantially increases, the

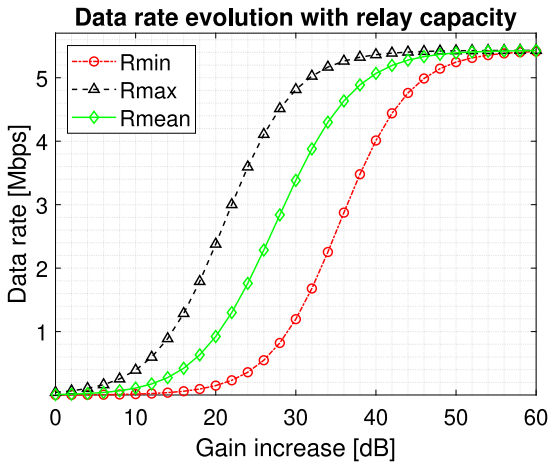

(a) Lagrange-relays network topology, consecutive model

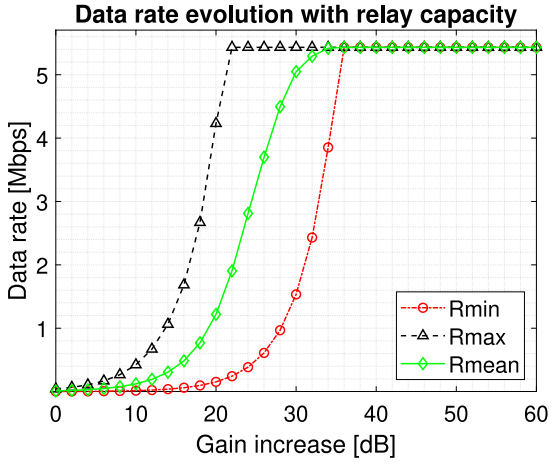

(b) Lagrange-relays network topology, simultaneous model

Fig. 12. Maximum, minimum and mean bit rate progression with the relay antenna's gain increase in the Lagrange-relays network topology, for both the consecutive and the simultaneous communication strategies.

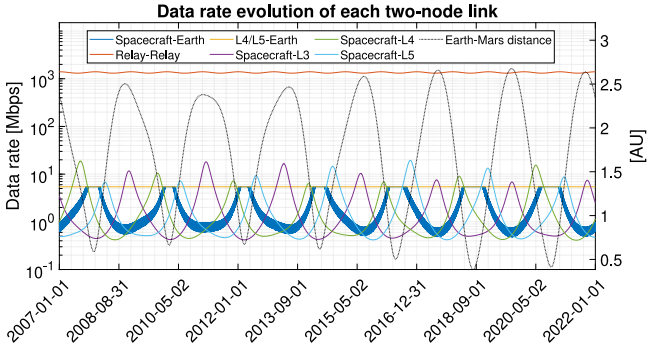

Fig. 13. Evolution of each simple link involved in the Lagrange-relays network topology, with an assumed gain increase of the relays of 25 dB.

link between the spacecraft and the relay strengthens whilst the link between the relay and Earth starts to become bounded by its own restrictions. This eventually leads to a homogenization of the bit rate prospects (see blue and green evolution in the figure below), reaching an asymptotic value, as previously discussed in the analysis of the bit rate improvements with the relay's gain increase. Therefore, when the relay capabilities improve, the relay's optimal orbit size indeed

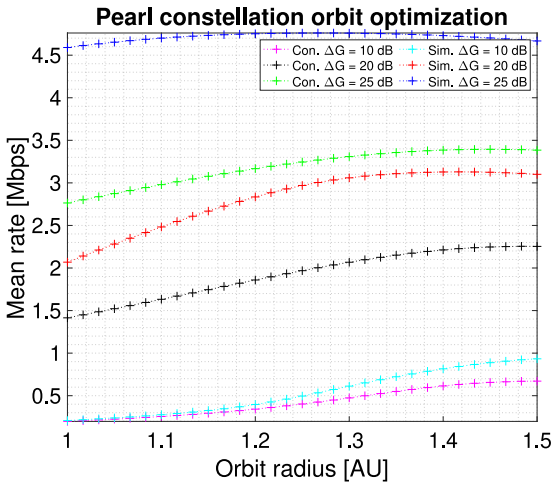

Fig. 14. Pearl constellation (N = 4) optimization analysis with relay antenna's gain increase.

decreases, but the evolution evens itself up to a point where the orbit size does not matter anymore because bit rate is always the same.

In consequence, the analysis of bit rate progression with the increased relay capabilities can be performed at the current orbit size (i.e., 1.4 AU) with a small loss of generalization. The evolution of minimum, maximum and average values of the pearl constellation bit rate evaluated over a period of 2 years versus the relay antenna's gain increase is presented in Fig. 15. Certainly, the only range where orbit is not optimized can be seen in the simultaneous evolution of the pearl constellation in Fig. 15, where the range [15, 35] dB shows a slower enhancement because the orbit is in fact not optimized. When compared to the Lagrange-relays evolution, the pearl constellation reaches the DSN constraint earlier (at least the peak values evolution) because of the shorter distance between the spacecraft and the relays, which has been found to be the bottleneck of the network. Finally, the 20 dB gain increase in the relays is chosen for the pearl constellation case.

In Fig. 16, the evolution of each possible link over a time period of 15 years in the pearl constellation topology with the stated improvement is presented. Analogously to the Lagrange-relays network topology, the peak values show a progression that results from the changes in the Earth–Mars geometry, but in all cases these lie in a range of values that is equivalent to – if not outperforming – the DTE link. On the other side, and as described before, since their orbit is bigger when compared to the Lagrange relays, the frequency of the peaks is smaller. Every 2 years or so, the relays switch their leading roles for the Earth–Mars communications, leaving the others as an alternative option in case the closest relay to Mars is not available (nor the DTE link).

As a final remark, it has been previously explained that when the relays present state-of-the-art telecommunication hardware, the link between the spacecraft and the relays permanently becomes the bottleneck of the communication between Earth and Mars (see Fig. 11). But, in a more complex situation, such as the case where the intermediary relay is not able to communicate with Earth and therefore another relay must forward the message, another bottleneck – even worse than the preceding one – may appear: limited link capacity between the relays. Fortunately, this issue is more sensitive to the improvements that a gain increase provides, i.e., the reduction of such bottleneck will be better than that of the link between the spacecraft and the relay, as the antenna's gain is increased at the two ends (both at the transmitter and the receiver). In effect, taking a look at Figs. 13 and 16, it is seen that the link between the relays stands out from the other ones, leading those complex situations that formerly involved the worst case scenario

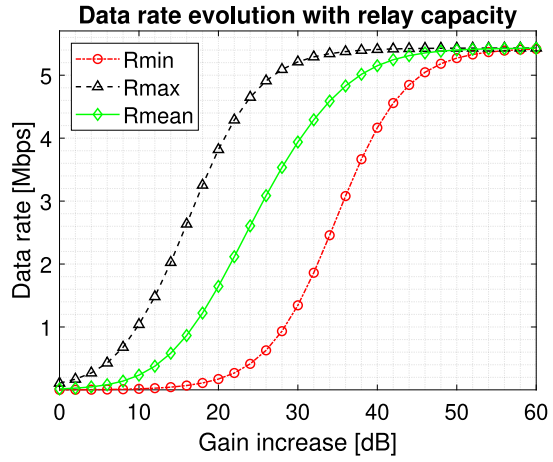

(a) Pearl constellation with 4 satellites, consecutive model

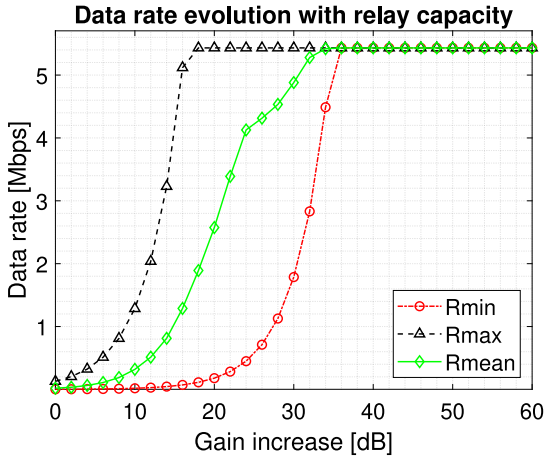

(b) Pearl constellation with 4 satellites, simultaneous model

Fig. 15. Maximum, minimum and mean bit rate evolutions with the relay antenna's gain increase in the Lagrange-relays and pearl constellation network topologies, for both the consecutive and the simultaneous communication strategies.

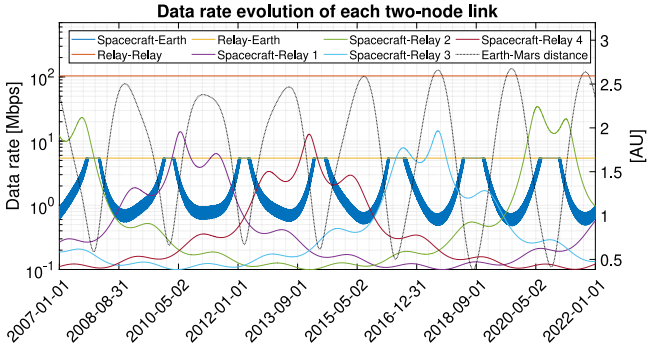

Fig. 16. Evolution of each simple link involved in the pearl constellation topology, with an assumed gain increase of the relays of 20 dB.

to a reasonable and practicable alternative, with no negative impact on the overall bit rate.

As stated before, the number of relays for this study has an arbitrary value, as the effect of an increase of the number of relays in the pearl constellation can be directly inferred from the results of the former. First of all, a higher number of relays would reduce the distance and consequently enhance the communication bit rate between them. Secondly, the period for exchanging the leading role would also be

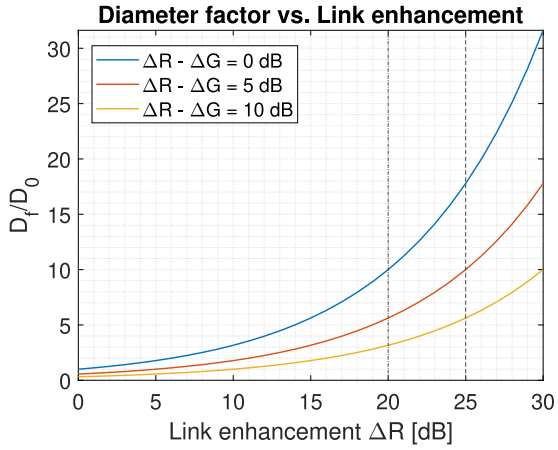

Fig. 17. Diameter increase factor evolution with link enhancement and different allocations of telecommunication system upgrades. The black dotted lines correspond to the obtained link increase for both network topologies. (For interpretation of the references to color in this figure legend, the reader is referred to the web version of this article.)

decreased, as the spacecraft could find a closer relay in a shorter time. This also means that some of the relays that are next to the closest one would not be that far from the spacecraft, bringing a reasonable alternative for those situations where the leading one is not available. Last but not least, the frequency of the peaks within the bit rate evolution over the 2-year period would grow and, as a consequence, so would the mean value of the overall evolution.

All in all, the necessary enhancement coming from the telecommunication parameters in order to bring each of the proposed network topologies' performance closer to that of the DTE link with the DSN has been settled to 20 dB and 25 dB for the pearl constellation and Lagrange-relays topology, respectively. So far, this enhancement has been regarded as antenna's gain increase. In terms of relay design, this might relate to a diameter swell of the antenna according to $G \propto D^2$, where D is the antenna diameter. Nevertheless, there are other ways to upgrade the link performance such as enhancing power transmission, improving the receiver's sensitivity or obtain a gain by codification. As a matter of fact, any of the aforementioned improvements have direct but different impacts on the bit rate increase. Just as a diameter swell would lead to a gain upgrade both for the transmission and the reception, the power transmission, for instance, would only affect the first. Fig. 17 presents the diameter multiplication factor with the link enhancement caused by a gain increase of the relay's antenna. In addition to this, the figure shows the influence on diameter multiplication if the total link enhancement was allocated among other parameters from the telecommunications system – besides antenna's gain – in different proportions. As it can be seen, if the resolved link enhancement was translated entirely into gain upgrade, the resulting relay diameter multiplication factors would be 10 and 17.9 for the pearl constellation and Lagrange-relays network topology, respectively. However, with an increment allocation of 10 dB in other parameters, these values could be brought down to 3.2 and 5.6, respectively.

To conclude, Fig. 18 shows the analogous bit rate progressions presented in Fig. 8 and Fig. 10, this time with an increased relay antenna's gain of 25 dB and 20 dB, respectively. For the sake of simplicity, only one DSN antenna (DSS-45) has been enabled. Fig. 18(a) and (b) show the consecutive and simultaneous progressions for the Lagrange-relays network topology, whilst Fig. 18(c) and (d) show the analogous for the pearl constellation topology with 4 satellites. These evolutions represent the intended objective of this study: a scenario where the proposed topologies enable an enhancement to the overall Earth–Mars communications in terms of bit rate (besides availability, discussed earlier). On the whole, it can be observed in the figures

that during the time period where Earth is found at the furthest distances from Mars and hence the bit rate is significantly reduced – i.e., from January 2017 to almost March 2018, approximately 60% of the synodic time period–, both the Lagrange-relays and the pearl constellation can take over and provide greater bit rate values than the DTE link. Indeed, during the aforementioned time window, while the DTE link may not exceed 1.5 Mbps, the proposed network topologies can forward at a bit rate comprised between 1 and 5.5 Mbps. This enhancement of MRO-DSN communications is especially striking during superior solar conjunctions. As explained earlier, this inconvenient phenomena implies the bothersome solar interference (RFI), which can significantly deteriorate the link performance, but, in addition to this, Earth and Mars also happen to be at their maximum distance, which is a significant drawback for the communication itself due to path loss. During the time period that goes from 2017 to 2019, there is a superior solar conjunction between Earth and Mars from July 17th, 2017 to August 5th, 2017. In fact, even if the Sun would not interfere in this communication, the available bit rate would be very small (max. 500 kbps), and this also applies to the surroundings around this ephemeris, where the bit rate is always below 1 Mbps during a non-negligible amount of time – over a year – due to the increased distance that makes path loss greater. In contrast, the Lagrange-relays and pearl constellation network topologies may successfully avoid the RFI and shorten path loss to enable bit rates of up to 5.5 Mbps –in the case of the pearl constellation topology. Note that the communication through the relays is not exempt of solar conjunctions. Taking a closer look at Fig. 18(c), see the interruption of the communication between the MRO and the DSS-45 through relay R_3 caused by a solar conjunction between the relay and Earth –that is in fact overlapping with a superior solar conjunction between Earth and Mars– from July 25th, 2017 to August 20th, 2017. Fortunately, though, the network topology is able to offer other possible routes with very similar bit rates that help to cope with the circumstances.

What is more, the combination of enhanced availability and bit rate leads to a third improvement: data volume. Calculating data volume as the integral of the bit rate over the Martian synodic period, the DTE evolution – with one DSN station – enables a total data downlink of 5.95×10^1 Tb whilst the Lagrange-relays and the pearl constellation network topologies, over that same period, may raise that number up to 1.8×10^2 Tb and 2×10^2 Tb, respectively; in other words, the total scientific return of MRO per DSN antenna may be increased up to 3 times, approximately.

5. Conclusions

The future of deep space communications encompasses a challenging situation where the current facilities used to communicate with different spacecraft may become saturated as a result of an increasing number of missions and their complexity. In this situation, increased communication availability and link performance between the communicating nodes would have a major impact. For this reason, this study proposes to locate deep space relays at strategic locations – i.e., building a network topology – that could make a difference for the deep space communications prospects, more specifically, Earth and Mars.

Therefore, this paper aims to quantitatively analyze current and future Earth–Mars communications by developing SolarCom, a software tool that allows to compute availability, bit rate and even the best communication route – in case there are more than two communicating nodes involved – between a Martian orbiter and a DSN ground station, at any time. As a matter of fact, provided the location and the telecommunication system parameters of the communicating nodes, SolarCom may be readily scalable to any other scenario besides Earth–Mars. This means that other spacecraft could be brought into the equation, but also other network topologies could be assessed (even for Earth–Mars communications).

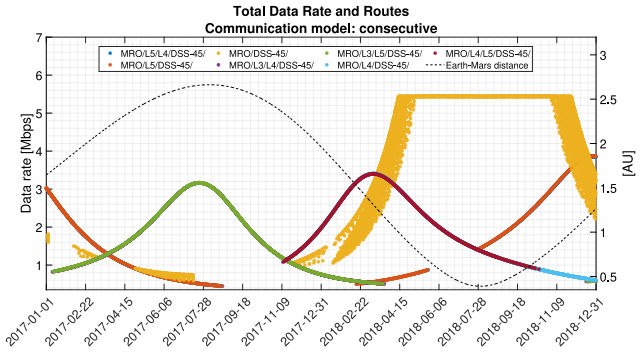

(a) Lagrange-relays network topology. Consecutive model.

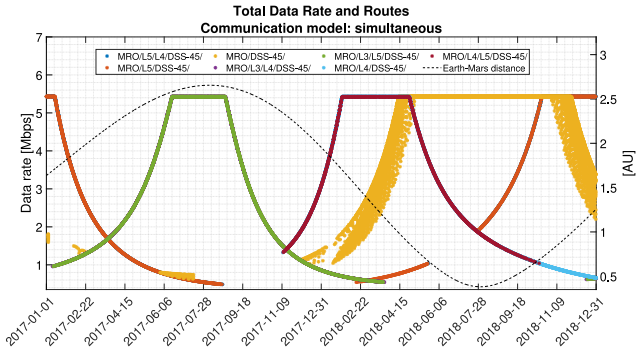

(b) Lagrange-relays network topology. Simultaneous model.

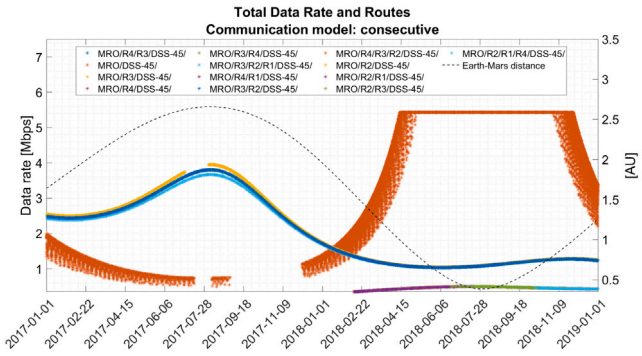

(c) Pearl constellation. Consecutive model.

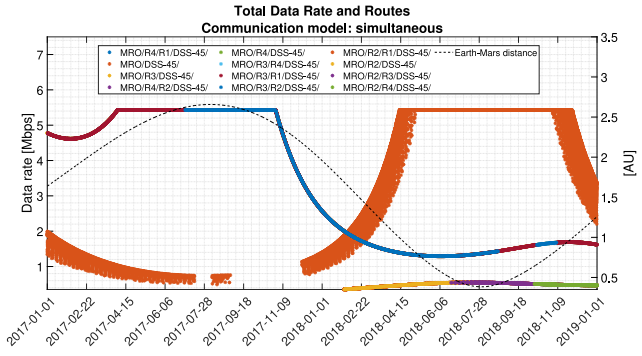

(d) Pearl constellation. Simultaneous model.

Fig. 18. Bit rate evolution of MRO communications with Earth's 34 m DSN antenna DSS-45 with improved relay design. Both the consecutive and simultaneous outcomes are shown for both network topologies.

This study has proved that the network topology proposals are indeed an advantageous option to significantly increase the availability of Earth–Mars communications. Indeed, whilst the DTE link availability between the MRO and any DSN antenna is no more than 70% during the Martian synodic period, the pearl constellation, instead, may provide with up to 100% of communication availability, followed up close by the Lagrange-relays network topology with a 91%. Furthermore, this availability increase affects also superior solar conjunctions, which can be successfully avoided by means of the relays. This is a significant advantage for future manned missions that will not allow any disruption on the communication but also for the existing missions, as solar conjunctions usually lead to troublesome interruptions of the orbiters and rovers' normal activity on Mars. On the other side, the availability enhancement is especially salient in the one-antenna case, which has a direct impact on the robustness of deep space communications: if one or two of the three DSN facilities would become inaccessible, the remaining antennas would be able to cope with most of the mission workload.[11] Giving another point of view to the latest statement, having that much communication availability with only one antenna could enable ground stations – other than the DSN – to boost their communications with Mars.

Nevertheless, from the bit rate point of view, this potential is strongly constrained by the telecommunication hardware development in the short-term future as the currently attainable relay capabilities – based on TDRSS technology [31] – cannot outweigh the performance of the DSN, even at short distances. Therefore, an analysis on improved relay capabilities and their impact on the resulting bit rate evolution has been performed, setting a realistic boundary and direction to which future telecommunication system developments should be aiming for. All things considered, it has been shown that the relays must display at least a 25 dB and 20 dB increase on antenna's gain in the Lagrange-relays and pearl constellation topologies, respectively, in order to become a comparable solution to the DTE link. Thus, the final landscape shows that during those time periods where Earth and Mars are farthest away from each other and the DTE link cannot offer any more than a bit rate of 1.5 Mbps, the communication via relays, conversely, may raise this value up to 5.5 Mbps, and no less than 1 Mbps. The resulting diameter swell of the relay antennas is significant when assuming that the total link enhancement is entirely translated into antenna's gain. Instead of enlarging the antenna's dimension, the necessary directivity could possibly be obtained through antenna arrays or by upgrading the illumination efficiency of the antennas. Nevertheless, there are other options in the relay design space that may improve link performance, such as the transmission power, which could be enhanced by enabling the usage of high-performance amplifiers and signal processing. Moreover, the minimum SNR considered for the relays in this study was reasonably conservative. This parameter could readily be reduced by using state-of-the-art low noise amplifiers and demodulators. Lastly, another factor that could considerably improve the overall performance of the radio-links is the use of error-correcting algorithms.

Therefore, overall, these network topologies could indeed help deep space communications cope with future demands through the increased number of communication windows, enhanced bit rates and, ultimately, higher data volume that could be retrieved from the Martian orbiters (and/or landers). It has been calculated that the total science return from Mars via MRO could be tripled by any of the proposed networks.

Note that benchmarking the Lagrange-relays and pearl constellation network topologies against each other is kept out of the scope of this study as other meaningful factors – such as station-keeping costs or orbit insertion and stability – should be brought to consideration when analyzing their suitability.

As a final remark, it is worth mentioning that the Deep Space Network has still some headroom that could benefit both the DTE link and new network topologies. As a matter of fact, the DSN has already undertaken actions to widen its spectrum of communication band [38], i.e., to include the Ka-band as a nominal frequency of communication with the spacecraft. In fact, MRO already communicated with the DSN through Ka-band during its primary science mission phase between 2008 and 2010 [6]. The Ka-band entails higher space losses but also enlarged channel bandwidths, which might lead to a compromise solution between those factors that actually enhance the current capacities of the DSN in the short distances, especially in the Earth–Mars communications case, either directly or through strategically-located relays.

In regards to future endeavors, this study has considered only RF telecommunications as these are the state-of-the-art technology used in deep space communications. On the other hand, optical links, a very promising alternative that could bring telecommunications to a new performance level, is currently being studied and integrated to SolarCom in order to perform an analogous analysis to the one conducted in this paper. In this framework, the proposed network topologies could also be reinforced by the usage of geostationary satellites to relay communications with Earth, as Matriciani [33] proved to provide with meaningful improvements. Another effort that could be brought into consideration is to integrate SolarCom into a scheduling software, such as S^3, a tool that allows to elaborate a communications plan for the DSN through a multi-user collaborative environment [39]. Hence, the resulting software would allow to program the DSN facilities, provided the link performance scenario (as well as the optimal path) at any time and considering all the interacting users and missions. To that purpose, the search algorithm would need to consider the rate of the antenna to change pointing and penalize small communication windows (it may not be worth it for the antenna to change pointing). Additionally, the software could also evaluate other factors and influences when obtaining the optimal end-to-end path, such as buffering, spacecraft resources limitations or program restrictions.

Declaration of competing interest

The authors declare that they have no known competing financial interests or personal relationships that could have appeared to influence the work reported in this paper.

Acknowledgments

We thank Jim Taylor (Jet Propulsion Laboratory) for providing meaningful contributions to this work.

References

[1] R.J. Cesarone, D.S. Abraham, L.J. Deutsch, Prospects for a next-generation deep-space network, Proc. IEEE 95 (10) (2007) 1902–1915, http://dx.doi.org/10.1109/JPROC.2007.905043.

[2] A. Konsgen, A. Forster, Current state and future challenges in deep space communication: A survey, It - Inf. Technol. 63 (4) (2021) 219–234, http://dx.doi.org/10.1515/itit-2021-0002.

[3] M.A. Marcinkowski, S.T. Bell, P.G. Roma, The nature of conflict for teams in isolated, confined, and extreme environments, Acta Astronaut. 181 (2021) 81–91.

[4] D. Morabito, R. Hastrup, Communicating with mars during periods of solar conjunction, in: IEEE Aerospace Conference Proceedings, 3, (July) 2002, pp. 1271–1281, http://dx.doi.org/10.1109/AERO.2002.1035260.

[5] D.D. Morabito, S. Shambayati, S. Finley, D. Fort, The Cassini May 2000 solar conjunction, IEEE Trans. Antennas and Propagation 51 (2) (2003) 201–219, http://dx.doi.org/10.1109/TAP.2003.809055.

[6] J. Taylor, D.K. Lee, S. Shambayati, Mars reconnaissance orbiter Telecommunications, in: DESCANSO Design and Performance Summary Series, 2015, pp. 193–250, http://dx.doi.org/10.1002/9781119169079.ch6.

[11] This statement does not take into account DSN scheduling nor spacecraft resource concerns to perform such communications

[7] J. Quade, A. Anabtawi, S. Thomas, S. Laubach, Communications with curiosity during solar conjunction, in: IEEE Aerospace Conference Proceedings, 2020, pp. 1–9, http://dx.doi.org/10.1109/AERO47225.2020.9172557.

[8] P.E. Schmid, Lunar Far-side Communication Satellites, Tech. rep., Goddard Space Flight Center Greenbelt, Md., NASA, 1968, pp. 1–24.

[9] M. Wittig, Data relay for earth, moon and mars missions, in: 2009 International Workshop on Satellite and Space Communications, 2009, pp. 300–304, http://dx.doi.org/10.1109/IWSSC.2009.5286358.

[10] K. Bhasin, J.L. Hayden, Developing architectures and technologies for an evolvable NASA space communication infrastructure, in: A Collection of the 22nd AIAA International Communications Satellite Systems Conference and Exhibit Technical Papers, vol. 2, (May) 2004, pp. 1180–1191, http://dx.doi.org/10.2514/6.2004-3253.

[11] A. Alhilal, T. Braud, P. Hui, The Sky is NOT the Limit Anymore: Future Architecture of the Interplanetary Internet, IEEE Aerosp. Electron. Syst. Mag. 34 (8) (2019) 22–32, http://dx.doi.org/10.1109/MAES.2019.2927897.

[12] J.C. Breidenthal, M.C. Jesick, H. Xie, C.W. Lau, Deep space relay terminals for mars superior conjunction, in: 15th International Conference on Space Operations, 2018, (June) 2018, pp. 1–16, http://dx.doi.org/10.2514/6.2018-2424.

[13] D. Modenini, A. Locarini, L. Valentini, A. Faedi, P. Tortora, D. Rovelli, N. Mazzali, M. Chiani, E. Paolini, Two-leg deep-space relay architectures: Performance, challenges, and perspectives, IEEE Trans. Aerosp. Electron. Syst. 58 (2022) 3840–3858.

[14] J.D. Strizzi, J.M. Kutrieb, P.E. Damphousse, J.P. Carrico, Sun-Mars libration points and Mars mission simulations, Adv. Astronaut. Sci. 108 I (2001) 807–822.

[15] M. Jesick, Mars trojan orbits for continuous earth-mars communication, J. Astronaut. Sci. 67 (3) (2020) 902–931, http://dx.doi.org/10.1007/s40295-019-00195-y.

[16] M. Rahman, M. Islam, R. Huq, Deep space communication and exploration of solar system through inter- Lagrangian data relay satellite constellation deep space communication and exploration of solar system through inter-Lagrangian data relay satellite constellation, in: Proceedings of ICubeSat 2019, the 8th Interplanetary CubeSat Workshop, Milan, Italy, (June) 2019.

[17] P. Wan, Y. Zhan, X. Pan, Solar system interplanetary communication networks: architectures, technologies and developments, Sci. China Inf. Sci. 61 (4) (2018) http://dx.doi.org/10.1007/s11432-017-9346-1.

[18] Y. Jiang, G. Li, G. Zhang, S. Yang, The Hierarchical-Cluster topology control strategy of InterPlaNetary internet backbone based on libration points, in: Przegląd Elektrotechniczny (Electrical Review), 88, 2012, pp. 271–276.

[19] S.S. Limaye, I.D. Kovalenko, Monitoring Venus and communications relay from Lagrange Points, Planet. Space Sci. 179 (August) (2019) 104710, http://dx.doi.org/10.1016/j.pss.2019.104710.

[20] T.G. Howard, An initial design assessment for a communications relay satellite to support the interplanetary information infrastructure, in: 16th AIAA International Communications Satellite Systems Conference, 1996, pp. 566–575, http://dx.doi.org/10.2514/6.1996-1057.

[21] S. Haque, A Broadband Multi-hop Network for Earth-Mars Communication using Multi-purpose Interplanetary Relay Satellites and Linear-Circular Commutating Chain Topology, (January) 2011, pp. 1–28, http://dx.doi.org/10.2514/6.2011-330.

[22] P. Wan, Y. Zhan, A structured Solar System satellite relay constellation network topology design for Earth-Mars deep space communications, Int. J. Satell. Commun. Netw. 37 (3) (2019) 292–313, http://dx.doi.org/10.1002/sat.1287.

[23] K. Bhasin, J.L. Hayden, O. Scott Sands, Relay station based architectures and technology for space missions to the outer planets, AIAA (May) (2002) 1–6.

[24] G. Araniti, N. Bezirgiannidis, E. Birrane, I. Bisio, S. Burleigh, C. Caini, M. Feldmann, M. Marchese, J. Segui, K. Suzuki, Contact graph routing in DTN space networks: Overview, enhancements and performance, IEEE Commun. Mag. 53 (3) (2015) 38–46, http://dx.doi.org/10.1109/MCOM.2015.7060480.

[25] NAIF, SPICE, An Observation Geometry System for Space Science Missions, 2020, https://naif.jpl.nasa.gov/naif/index.html. (**Online**; accessed February 27th, 2020).

[26] C. Chang, DSN Telecommunications Link Design Handbook, (810-005 Rev. E) 2000.

[27] D.D. Morabito, Spectral broadening and phase scintillation measurements using interplanetary spacecraft radio links during the peak solar cycle 23, Radio Sci. 44 (2009).

[28] NASA, Mars MAVEN Orbiter https://mars.nasa.gov/maven/. (**Online**; accessed January 28th, 2022).

[29] M. Baldi, F. Chiaraluce, N. Maturo, G. Ricciutelli, A. Ardito, F. Barbaglio, S. Finocchiaro, L. Simone, R. Abelló, J.D. Vicente, M. Mercolino, End-to-end simulations of coded transmissions in space links affected by solar scintillation, IEEE Trans. Aerosp. Electron. Syst. 56 (4) (2020) 3259–3275, http://dx.doi.org/10.1109/TAES.2020.2970733.

[30] A.B. Carlson, P.B. Crilly, Communication Systems: An Introduction To Signals and Noise in Electrical Communication, fifth ed., McGraw-Hill, 2010.

[31] M. Toral, G. Heckler, P. Pogorelc, N. George, K. Han, Payload performance of third generation tdrs and future services, in: 35th AIAA Int. Commun. Satell. Syst. Conf. ICSSC 2017, 2017.

[32] H. Monaghan, Tracking and data relay satellite (TDRS), 2015, URL http://www.nasa.gov/directorates/heo/scan/services/networks/tdrs_main#.Yd23oRmeXKk.mendeley.

[33] E. Matricciani, Deep–space communications with a 2–hop downlink with high availability, Int. J. Satell. Commun. Netw. 23 (2005) 203–228, http://dx.doi.org/10.1002/sat.815.

[34] R.M. Gagliardi, Satellite Communications, Springer Science & Business Media, 2012.

[35] E.W. Dijkstra, A note on two problems in connexion with graphs, Numer. Math. 1 (1) (1959) 269–271, http://dx.doi.org/10.1007/BF01386390.

[36] C. Vallat, N. Altobelli, B. Geiger, B. Grieger, M. Kueppers, C. Muñoz Crego, R. Moissl, M.G. Taylor, C. Alexander, B. Buratti, M. Choukroun, The science planning process on the Rosetta mission, Acta Astronaut. 133 (March 2016) (2017) 244–257, http://dx.doi.org/10.1016/j.actaastro.2017.01.018, URL http://dx.doi.org/10.1016/j.actaastro.2017.01.018.

[37] NAIF, NAIF Integer ID codes. https://naif.jpl.nasa.gov/pub/naif/toolkit_docs/FORTRAN/req/naif_ids.html. (**Online**; accessed January 28th, 2022).

[38] R. Labelle, D. Rochblatt, Ka-band high-rate telemetry system upgrade for the NASA deep space network, Acta Astronaut. 70 (2012) 58–68, http://dx.doi.org/10.1016/j.actaastro.2011.07.023.

[39] M.D. Johnston, D. Tran, B. Arroyo, S. Sorensen, P. Tay, B. Carruth, A. Coffman, M. Wallace, Automating mid- and long-range scheduling for NASA's Deep Space Network, in: SpaceOps 2012 Conference, 2012, pp. 1–12, http://dx.doi.org/10.2514/6.2012-1296235.